Science Advances
◣AAAS

Supplementary Materials for

Shrinking dinosaurs and the evolution of endothermy in birds

Enrico L. Rezende*, Leonardo D. Bacigalupe, Roberto F. Nespolo, Francisco Bozinovic

*Corresponding author. Email: erezende@bio.puc.cl

This PDF file includes:

Comparison between Lee et al. (*22*) and Benson et al. (*15, 23*)

Body mass estimation

Lee et al (*22*) and Benson et al. (*15, 23*) employed different methods to estimate body mass from, respectively, femur length or femoral circumference (details in the Supplementary Material of Lee et al. (*22*) and Appendix S1 for Benson et al. (*23*). To ensure that body mass estimates were comparable, we plotted the values recalculated for the subset of species shared across studies against the 1:1 line, as shown below.

Estimates are very similar, and the only data point that deviates from the general relationship actually corresponds to a typo in Lee's dataset for *Piatnitzkysaurus floresi*: whereas in Lee's supplementary dataset the femur length was 152 mm (resulting in a 5.5 kg mass estimate), the appropriate femur length of 552 mm from Benson's dataset resulted in a mass estimate of 352 kg (red point in the attached figure). After correcting this typo, the regression between Lee's and Benson's estimate gave rise to an r-square = 0.9778 (fig. S1). Thus, the uncertainty associated with different methods to reconstruct body mass corresponds to slightly more than 2% of the total variation.

Importantly, Lee's reconstruction method seems to underestimate body mass at lower sizes, as evidenced by a regression slope that is slightly higher than 1 (slope = 1.102 ± 0.017 SE). Consequently, Lee et al. (*22*) might be overestimating the amount of miniaturization in smaller and more recent lineages such as Avialae. Nonetheless, our results remain qualitatively identical with both Lee's and Benson's dataset (below).
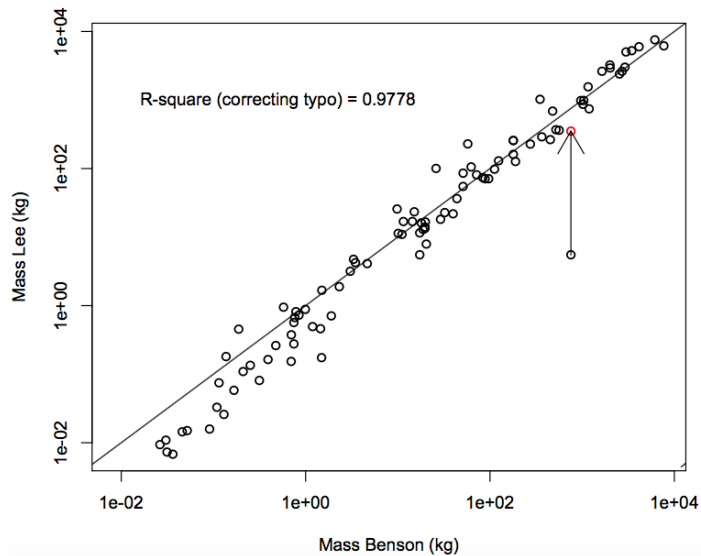

Fig. S1. Relationship between body size reconstructions performed by Benson *et al.* (*15, 23*) and Lee *et al.* (*22*). Note that we found a typo in Lee's dataset (see above) and corrected it before running the regression.

Topology

On the same token, the reconstruction of phylogenetic relationships between theropod taxa differed considerably between Lee et al. (*22*) and Benson et al. (*23*). Whereas Lee's theropod phylogeny was based almost entirely on scorings derived from the literature and Markov-Chain Monte Carlo Bayesian methods to establish phylogenetic relations, Benson's phylogeny was a composite tree compiled from recent, taxon-rich cladistic datasets (details available in the Supplementary Material of their studies). Once more, to ensure that results hold across datasets, we selected those species in common in both studies (n = 94) and compared their phylogenetic relationships according to Lee et al. (*22*) and Benson et al. (*23*).

To quantify the degree of similarity, we employed Baker's Gamma Index which is essentially a correlation index varying between – 1 and 1 (analysis implemented as described here: https://cran.r-project.org/web/packages/dendextend/vignettes/introduction.html#correlation-measures) and obtained a Gamma = 0.9625. Thus, the two phylogenies provide virtually the same information regarding the relationship between the subset of species that these studies have in common (fig. S2). Note that the phylogenetic structure is strikingly similar even when we did not attempt to maximize the degree of matching between phylogenies (we simply 'ladderized' them independently in R and the similarity becomes immediately apparent).
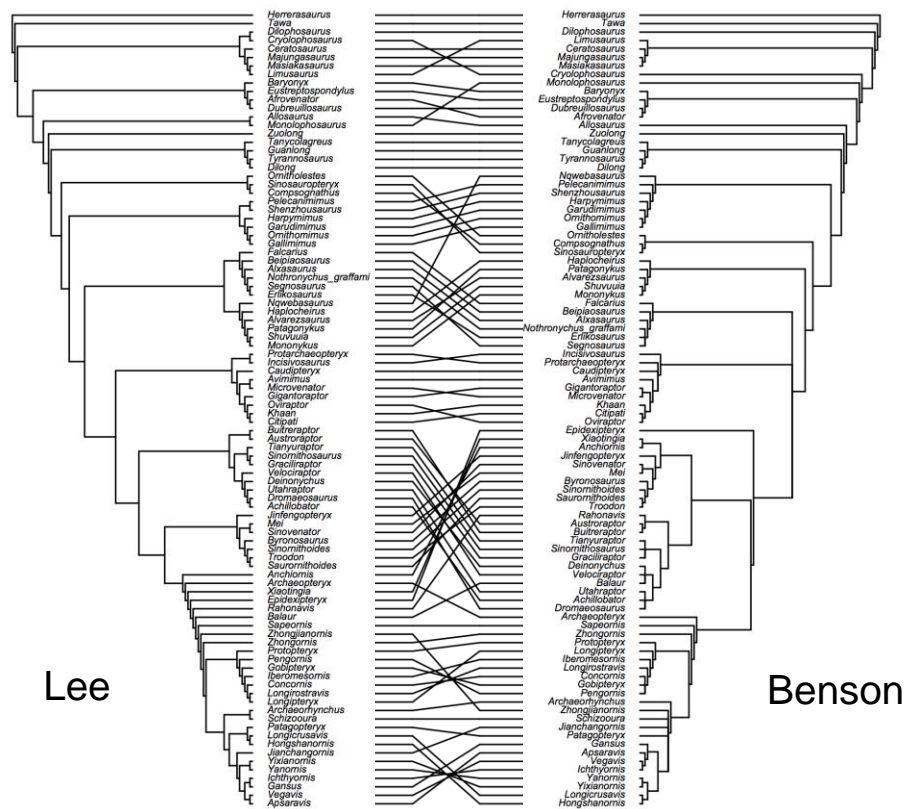

Fig. S2. Comparison between the topologies of the theropod phylogeny reconstructed by Lee *et al.* (*22*) and Benson *et al.* (*15*, *23*).

Calculations with Lee's dataset

We replicated analyses explained in the main text employing Lee's dataset, which has arguably two problems when compared with Benson et al. (*15*) and references therein: an overestimation of the ancestral size of the basal theropod and a gradual reduction in body size between paravians and Avialae. For consistency, analyses with the dataset by Lee et al. (*22*) assume that the basal theropod is the largest ancestor with ecothermic metabolic levels instead of Tetanurae, as in the original study (see Methods). Nonetheless, the general reconstruction of the evolution of metabolic levels along the bird stem lineage, and the overall scenario proposed in our study, remains largely unchanged (Figs. S3, S4 and S5).
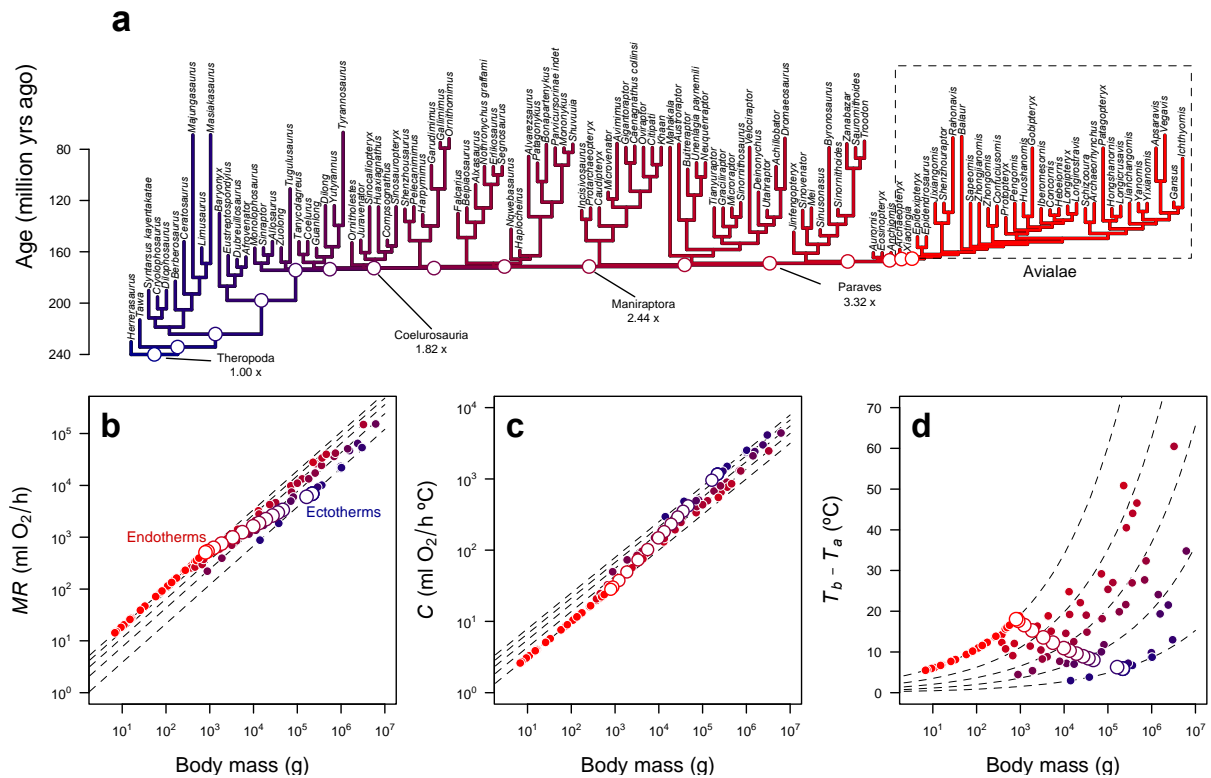
Fig. S3. Replicate of Fig. 2, except that, in this case, analyses were replicated using the dataset and phylogeny by Lee *et al.* (*22*).
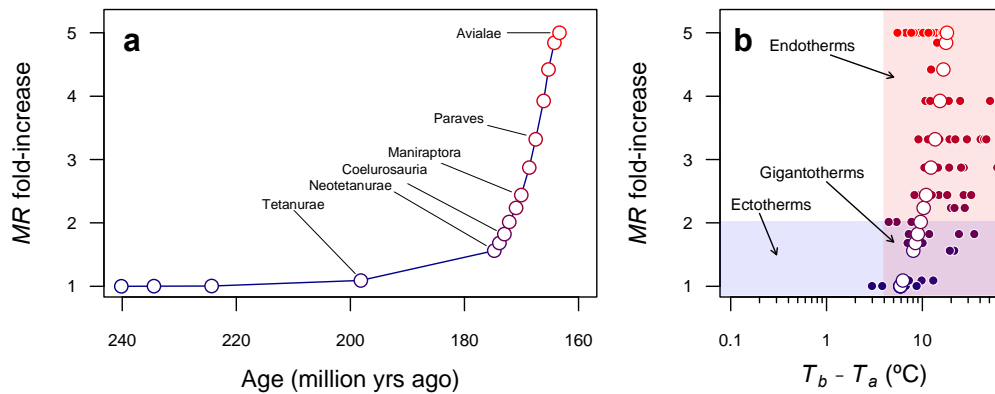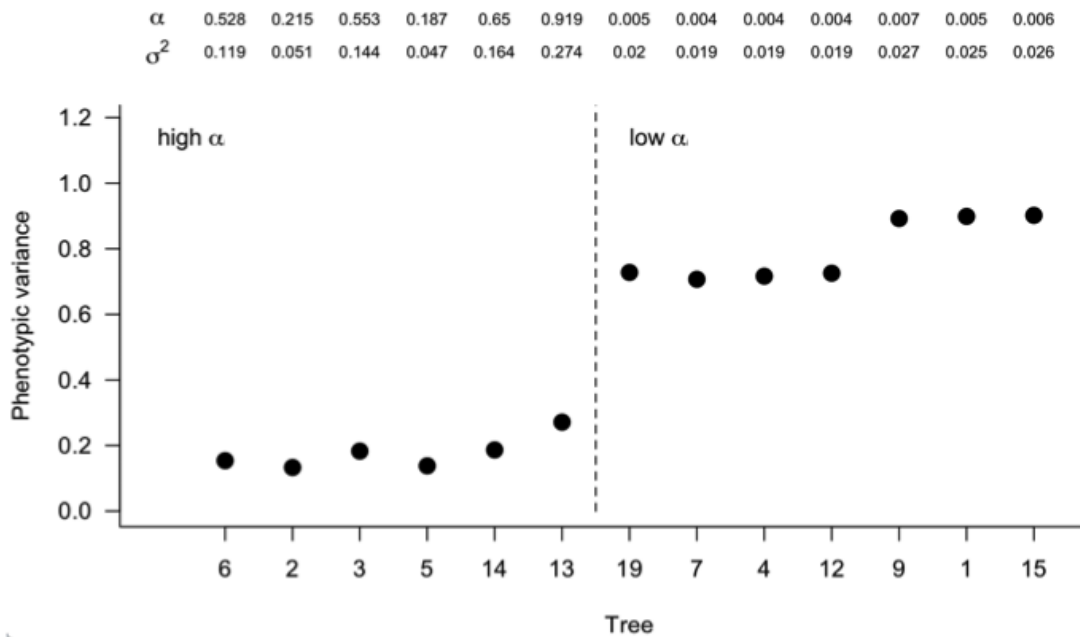
Fig. S4. Replicate of Fig. 4, except that, in this case, analyses were replicated using the dataset and phylogeny by Lee _et al._ (_22_).
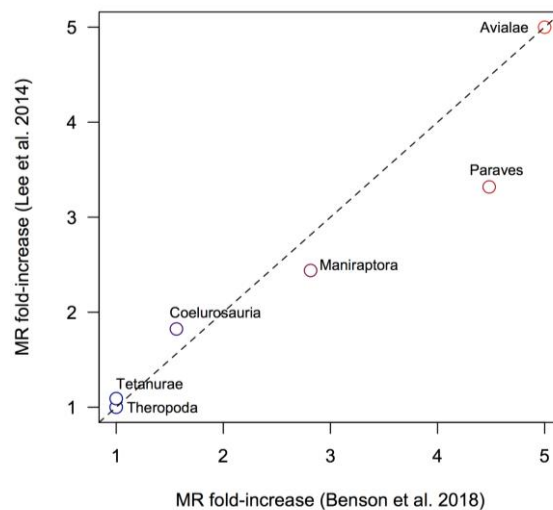
Fig. S5. Comparison between reconstructed metabolic levels along the bird stem lineage using the dataset by Benson _et al._ (_15_) and Lee _et al._ (_22_), plotted against the 1:1 line. As expected, estimates are highly correlated (Pearson $r_4 = 0.961$, 1-tailed P = 0.001). Note that the largest discrepancy is obtained for the Paraves node, which partly reflect a larger reconstructed body size for the paravian (~3.3 kg) and a smaller size for the Avialae common ancestor (~0.8 kg), respectively, reported by Lee et al. (_22_). In comparison, the estimates by Benson et al. (_15_) suggest a smaller paravian ancestor weighing around 1.4 kg and an avialan ancestor with a weight of 0.93 kg.

Null Model

We employed the parameters estimated by Benson et al. (*15*) in their Ornstein–Uhlenbeck (OU) models, fitted to the empirical distribution of theropod body size data from the fossil record, to simulate different evolutionary trajectories and obtain a null distribution of body sizes for both the ectothermic ancestor and endothermic descendant. Their analyses suggested complex patterns of body size evolution that fitted two broad classes of evolutionary models: OU models with high α and multiple adaptive peaks, which indicate that a large fraction of the observed phenotypic variance is dictated adaptive evolution towards different optima, and OU models with low α that suggest that this variation results primarily from random fluctuations in the evolutionary process (incidentally, in the extreme scenario where α = 0, the OU process converges to Brownian motion). The parameters and the resulting phenotypic variance expected from the random component in the different OU model reported by Benson et al. (*15*) are shown below (fig. S6), which shows that models with a single optima result in a higher phenotypic variation.

α	0.528	0.215	0.553	0.187	0.65	0.919	0.005	0.004	0.004	0.004	0.007	0.005	0.006
σ^2	0.119	0.051	0.144	0.047	0.164	0.274	0.02	0.019	0.019	0.019	0.027	0.025	0.026

Fig. S6. Phenotypic variance simulated with the difference parameters fitted by Benson *et al.* (*15*) for the theropod phylogeny (parameters available in their appendix S5).

For our null model, we selected parameters σ^2 and α from a single-optimum OU model because we want to simulate a process without directionality that is 'null' in that it has no additional explanatory factors such as different adaptive peaks. More specifically, we selected parameters from Tree 1 because simulations with $\sigma^2 = 0.025$ and $\alpha = 0.005$ gave rise to the highest phenotypic variance across trees and therefore the resulting body size distribution would correspond the most conservative null model (results remain qualitatively identical if other single-optimum OU models are selected instead).

Subsequently, we confirmed whether simulations employing the parameters fitted by Benson et al. (*15*) adequately mirrored the empirical distribution of body size across theropod lineages, as shown in the phenogram below (fig. S7).
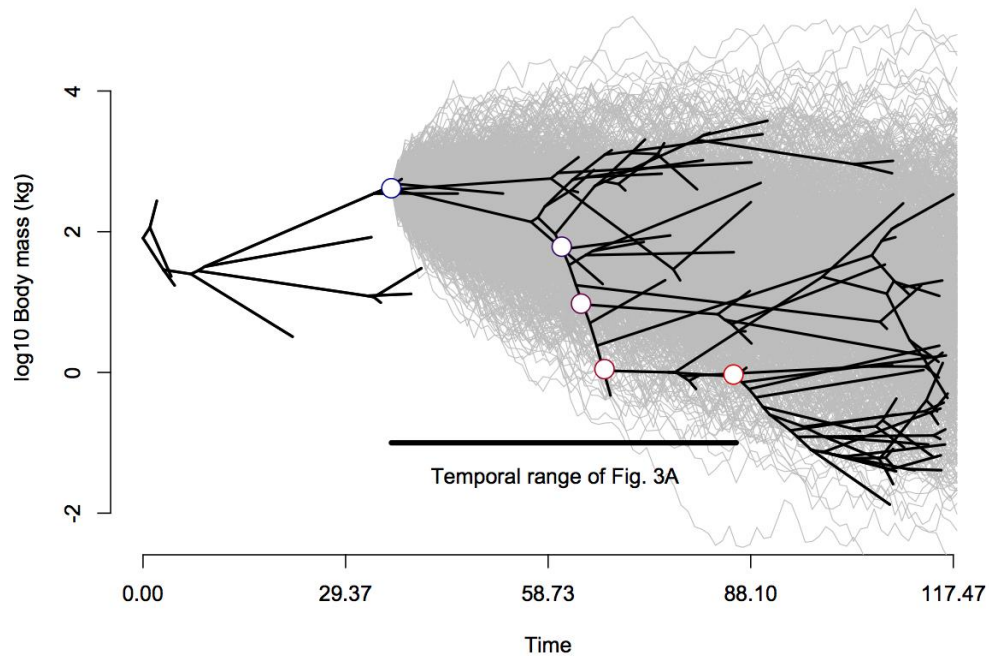

Fig. S7. Simulated OU model overlapped against the empirical data from Benson *et al.* (*15*) (their appendix S5), which shows that this model can replicate the distribution of phenotypic data observed along the theropod phylogeny and provide a valid "null model" in the absence of directionality (see below).

For the null model we removed the directional trend associated with $\theta = 45$ kg (the single adaptive peak that was smaller than the 370 kg Tetanurae root node) by setting $\theta = 370$ kg, effectively obtaining a null evolutionary process that could generate the body size distribution observed in the empirical dataset with no directionality. For comparison, we also set $\alpha = 0$ to determine whether results hold under a simple Brownian motion process. Results are virtually identical (fig. S8).
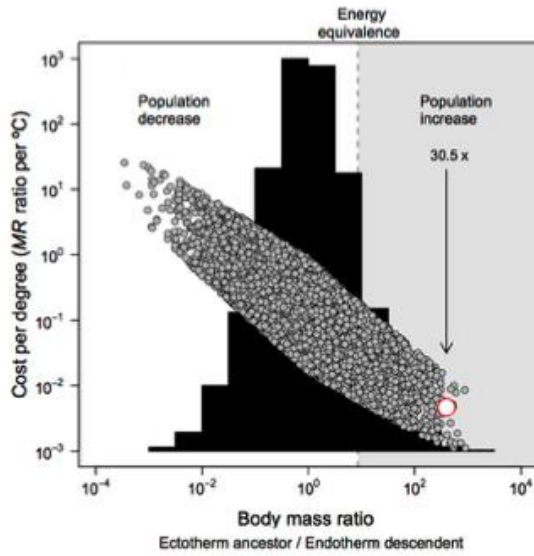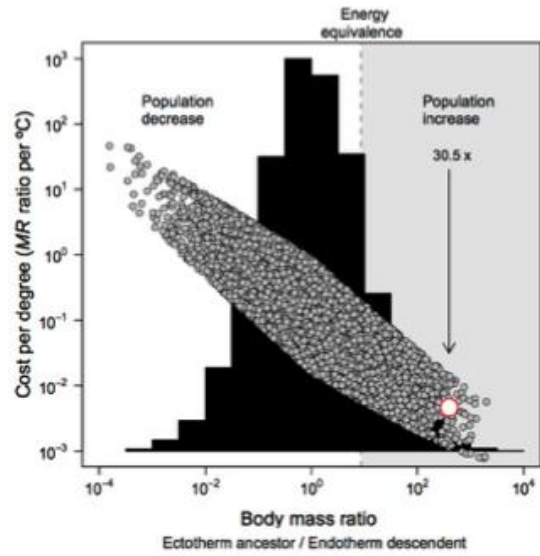
OU null model (Fig 3)   Brownian motion null model

Fig. S8. Results from the null model in the main text compared against expectations for a more conservative model assuming Brownian motion. Note that in both cases the reduction in size and estimation of energy costs fall in the tail of the distributions and are significantly different than the null distributions ($P < 0.05$).